Simulations and realizations of active right-handed metamaterials with negative refractive index

Bertil Nistad and Johannes Skaar

Department of Electronics and Telecommunications, Norwegian University of Science and Technology, NO-7491 Trondheim, Norway

bertil.nistad@iet.ntnu.no

Abstract: The theory of determining the sign of the refractive index in active materials is discussed. Animations of numerical simulations are presented, supporting the claim that negative refractive index may occur in right-handed media. An example of such a medium, in the form of a lumped circuit model with active and passive resonances, is presented.

OCIS codes: (160.4670) Optical materials; (160.4760) Optical properties; (260.2065) Effective medium theory; (260.2110) Electromagnetic optics; (350.4010) Microwaves; (260.2030) Dispersion.

References and links

1. V. G. Veselago, "The electrodynamics of substances with simultaneously negative ε and μ," Sov. Phys. Usp. **10**(4), 509–514 (1968).
2. J. B. Pendry, A. J. Holden, D. J. Robbins, and W. J. Stewart, "Low frequency plasmons in thin-wire structures," J. Phys.: Condens. Matter **10**(22), 4785–4809 (1998).
3. J. B. Pendry, A. J. Holden, D. J. Robbins, and W. J. Stewart, "Magnetism from conductors and enhanced nonlinear phenomena," IEEE Trans. Microwave Theory Tech. **47**(11), 2075–2084 (1999).
4. D. R. Smith, W. J. Padilla, D. C. Vier, S. C. Nemat-Nasser, and S. Schultz, "Composite medium with simultaneously negative permeability and permittivity," Phys. Rev. Lett. **84**(18), 4184–4187 (2000).
5. G. V. Eleftheriades, A. K. Iyer, and P. C. Kremer, "Planar negative refractive index media using periodically L-C loaded transmission lines," IEEE Trans. Microwave Theory Tech. **50**(12), 2702–2712 (2002).
6. S. A. Ramakrishna and J. B. Pendry, "Removal of absorption and increase in resolution in a near-field lens via optical gain," Phys. Rev. B **67**(20), 201101 (2003).
7. M. A. Noginov, G. Zhu, M. Bahoura, J. Adegoke, C. E. Small, B. A. Ritzo, V. P. Drachev, and V. M. Shalaev, "Enhancement of surface plasmons in an Ag aggregate by optical gain in a dielectric medium," Opt. Lett. **31**, 3022 (2006).
8. A. K. Popov and V. M. Shalaev, "Compensating losses in negative-index metamaterials by optical parametric amplification," Opt. Lett. **31**, 2169 (2006).
9. V. M. Shalaev, "Optical negative-index metamaterials," Nat. Photonics **1**, 41–48 (2007).
10. Y.-F. Chen, P. Fischer, and F. W. Wise, "Negative refraction at optical frequencies in nonmagnetic two-component molecular media," Phys. Rev. Lett. **95**(6), 067402 (2005).
11. J. Skaar, "Fresnel equations and the refractive index of active media," Phys. Rev. E **73**, 026605 (2006).
12. Y.-F. Chen, P. Fischer, and F. W. Wise, "Sign of the refractive index in a gain medium with negative permittivity and permeability," J. Opt. Soc. Am. B **23**, 45–50 (2006).
13. T. G. Mackay and A. Lakhtakia, "Comment on "Negative refraction at optical frequencies in nonmagnetic two-component molecular media"," Phys. Rev. Lett. **96**(15), 159701 (2006).
14. Y.-F. Chen, P. Fischer, and F. W. Wise, "Chen, Fischer, and Wise reply," Phys. Rev. Lett. **96**, 159702 (2006).
15. S. A. Ramakrishna, "Comment on "Negative refraction at optical frequencies in nonmagnetic two-component molecular media"," Phys. Rev. Lett. **98**(5), 059701 (2007).
16. Y.-F. Chen, P. Fischer, and F. W. Wise, "Chen, Fischer, and Wise reply," Phys. Rev. Lett. **98**(5), 059702 (2007).
17. S. A. Ramakrishna and O. J. F. Martin, "Resolving the wave vector in negative refractive index media," Opt. Lett. **30**, 2626 (2005).

#85000 - $15.00 USD Received 9 Jul 2007; revised 14 Aug 2007; accepted 14 Aug 2007; published 15 Aug 2007

18. A. N. Grigorenko, "Negative refractive index in artificial metamaterials," Opt. Lett. **31**, 2483 (2006).
19. J. Skaar, "On resolving the refractive index and the wave vector," Opt. Lett. **31**, 3372 (2006).
20. L. Brillouin, *Wave propagation and group velocity* (Academic Press, New York and London, 1960).
21. L. D. Landau and E. M. Lifshits, *Electrodynamics of continuous media*, chap. IX.62 (Pergamon Press, 1960).
22. In general, we can set $\gamma = 0^+$ provided the refractive index is analytic in the upper half-plane and the denominator in the Fresnel equations is nonzero in the upper half-plane. Excluding media with absolute instabilities, the refractive index can always be identified as an analytic function in the upper half-plane.
23. Poles in the upper half-plane mean that the slab will start lasing.
24. T. Koschny, P. Markos, E. N. Economou, D. R. Smith, D. C. Vier, and C. M. Soukoulis, "Impact of inherent periodic structure on effective medium description of left-handed and related metamaterials," Phys. Rev. B **71**(24), 245105 (2005).
25. B. Nistad and J. Skaar, in *Photonic metamaterials: From random to periodic*, V. M. Shalaev and A. Genack, eds. (OSA, 2006). ISBN:1-55752-808-X.
26. J.-S. Lee and Y.-S. Kwon, "Negative resistance circuit for monolithic resonators using gate-to-source resistive feedback," Electron. Lett. **34**(18), 1758–1760 (1998).
27. L. O. Chua, J. Yu, and Y. Yu, "Bipolar-JFET-MOSFET negative resistance devices," IEEE Trans. Circuits Syst. **31**(1), 46–61 (1985).
28. D. M. Pozar, *Microwave engineering*, chap. 4, 2nd ed. (Wiley, 1998).
29. M. Born and E. Wolf, *Principles of Optics*, chap. 1.6.5, pp. 66–67, 3rd ed. (Pergamon Press, 1965).

1. Introduction

In 1968 Veselago predicted that isotropic materials with simultaneously negative permittivity ε and permeability μ may yield negative refraction [1]. Veselago referred to such materials as left-handed due to the fact that the electric field, the magnetic field, and the wave vector constitute a left-handed set of vectors. Thus, the phase velocity and Poynting vector point in opposite directions, in contrast to the situation in right-handed materials. Left-handed materials do not exist naturally; however, it is possible to make artificial metamaterials with negative ε and μ in the same frequency range [2, 3, 4, 5].

Passive metamaterials often suffer from limited performance due to large losses. It has therefore been suggested to combine them with active gain media [6], or even create active metamaterials [7]. Nonlinear processes such as parametric amplification have also been suggested as a method for overcoming inherent losses in metamaterials [8]. As the interest in active metamaterials seem to be increasing [9], it is crucial to understand fundamentally how they behave electromagnetically.

Of particular interest are the sign of the refractive index (direction of phase velocity), and the direction of the energy flow. The sign of the refractive index depends on the location of zeros and poles of $\varepsilon\mu$ in the complex ω-plane. This indicates that it is possible to obtain negative refractive index without any magnetic resonances, $\mu = 1$, but instead two electric resonances. Indeed, it has been suggested that certain nonmagnetic media, with active and passive dielectric resonances, can exhibit negative refraction [10]. In such right-handed materials the wave vector and Poynting vector both point towards the source [11].

Recently, these results have been discussed in the literature [11, 12, 13, 14, 15, 16]. While the conclusions differ, all authors seem to argue that causality must determine the sign of the refractive index. However, the interpretations of causality differ and in fact, give different results for certain active media [10, 11, 12, 13, 14, 15, 16, 17, 18, 19]. To identify the correct interpretation and resolve this controversy, it is necessary to go back to first principles: Causality means that if an excitation starts at time $t = 0$, no effect can be detected a distance z away before $t = z/c$. In other words, the front of an electromagnetic wave cannot travel faster than c, the vacuum velocity of light [20]. Using this principle, it has been shown analytically how to determine the sign of the refractive index in active media [11].

In this work, we will first present animations of numerical simulations, to demonstrate negative refractive index in right-handed, active media [10, 11]. The electromagnetic solution in

#85000 - $15.00 USD Received 9 Jul 2007; revised 14 Aug 2007; accepted 14 Aug 2007; published 15 Aug 2007

a slab of thickness d can be found unambiguously as it only dependents on ε, μ, and d, and is independent of the refractive index. Moreover, by causality, *the time-domain solution for $t < d/c$ must be identical to that of a semi-infinite medium* when the slab is excited at one side, starting at $t = 0$. Letting d be sufficiently large, the solutions can be compared in an arbitrarily large time window. The movies clearly support the claim that negative refractive index may be obtained in active, right-handed media.

To concretize this class of media, we propose a 1-D transmission line model with lumped circuit elements, implementing a right-handed medium with negative refractive index. This model can be used as a starting point for analysis and possible implementation. Although we consider a one-dimensional structure, generalization to two dimensions is straightforward.

2. Determining the sign of the refractive index

When a plane wave is normally incident from vacuum to a semi-infinite medium, the reflection R and transmission S are given by the Fresnel equations:

$$R = \frac{\eta - 1}{\eta + 1}, \tag{1a}$$

$$S = \frac{2\eta}{\eta + 1} \exp(i\omega nz/c). \tag{1b}$$

Here $k = \omega n/c$, $\eta = \mu/n$, and $n^2 = \varepsilon\mu$; ε and μ are the permittivity and permeability of the semi-infinite medium. The interface between vacuum and the semi-infinite medium is the plane $z = 0$; the region $z > 0$ is the location of the semi-infinite medium. For convenience, the propagation factor $\exp(i\omega nz/c)$ is included in S. The sign of the refractive index n must be identified to ensure causality; for passive materials this can be achieved simply by requiring that the Poynting vector point in $+z$-direction, or that the wave decays in the $+z$-direction. As an example of an active medium, we consider a material with $\varepsilon(\omega) = (1 + f(\omega))^2$ and $\mu(\omega) = 1$, where

$$f(\omega) = \frac{F\omega_0^2}{\omega_0^2 - \omega^2 - i\omega\Gamma}. \tag{2}$$

We take $F = 2$ and $\Gamma = 0.005\omega_0$. This material is causal and realizable as ε is analytic in the upper half-plane of complex frequency and $\varepsilon(\omega) - 1 \sim -2F\omega_0^2/\omega^2$ as $\omega \to \infty$ [21]. Using the method of Refs. [20, 10, 11, 12, 19], we find the refractive index $n_1(\omega) = 1 + f(\omega)$. On the other hand, using the approaches in Refs. [13, 15, 17, 18], we find the refractive index $n_2(\omega) = (1 + f(\omega))\mathrm{Re}\,(1 + f(\omega))/|\mathrm{Re}\,(1 + f(\omega))|$. The real and imaginary parts of the refractive index for the two different solutions are plotted in Fig. 1. Note that there is a frequency band where $\mathrm{Re}\, n_1(\omega) < 0$; thus the first solution predicts that both phase velocity and steady-state energy flow may point towards the source. For the other solution, $\mathrm{Re}\, n_2(\omega) > 0$ for all frequencies; thus this solution means that the phase velocity and energy flow are directed away from the source. Note the two points, $\omega = \omega_0$ and $\omega = 1.73\omega_0$, where $n_2(\omega)$ is discontinuous.

To resolve the above controversy, we first compute the time-domain solutions associated with the choices $n_1(\omega)$ and $n_2(\omega)$. This is achieved with the inverse Laplace transform. We excite the medium by a plane wave, normally incident at $z = 0^-$, starting at $t = 0$. For example, if the excitation at $z = 0^-$ is $u(t)\cos(\omega_1 t)$, where $u(t)$ is the unit step function and ω_1 is the excitation frequency, the time-domain field in the material can be expressed as

$$E(z,t) = \frac{i}{2\pi} \int_{i\gamma-\infty}^{i\gamma+\infty} \frac{\omega S \exp(-i\omega t)}{\omega_1^2 - \omega^2}\, \mathrm{d}\omega. \tag{3}$$

#85000 - $15.00 USD Received 9 Jul 2007; revised 14 Aug 2007; accepted 14 Aug 2007; published 15 Aug 2007

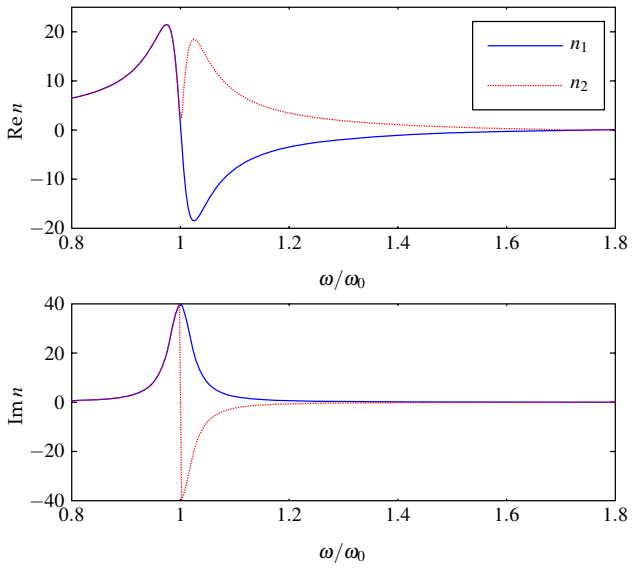

Fig. 1. Refractive index vs. frequency for the two choices $n_1(\omega)$ and $n_2(\omega)$.

Here γ is a sufficiently large, positive number, such that $\mathrm{Im}\,\omega < \gamma$ for all poles or nonanalytic points. For S given by Eq. (1b), assuming that the refractive index has meaning for real frequencies, the integral can be evaluated just above the real frequency axis ($\gamma = 0^+$) [11, 22]. The excitation frequency is taken to be $\omega_1 = 1.4\omega_0$; at this frequency $\varepsilon(\omega_1) \approx +1.13 - 0.32i$. Now we can examine the solutions associated with $n(\omega) = n_1(\omega)$ (Fig. 2) and $n(\omega) = n_2(\omega)$ (Fig. 3), and judge whether they satisfy causality. Note that causality should be interpreted in its most fundamental form; no field can arise at z before the time $t = z/c$. We clearly see that

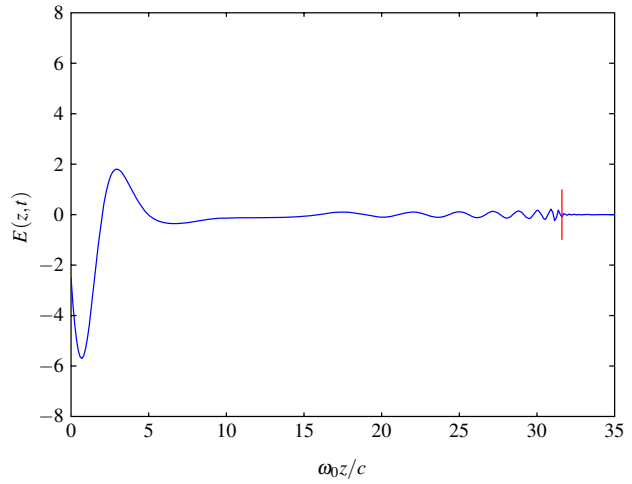

Fig. 2. Numerical simulation of the time-domain electric field $E(z,t)$ for a semi-infinite medium with refractive index $n(\omega) = n_1(\omega)$ and excitation frequency $\omega_1 = 1.4$. The excitation, $\cos(\omega_1 t)$, is initiated at $t = 0$. After roughly a time $70/\omega_0$ the steady-state solution (monochromatic solution) has been built up. The excitation is turned off at $t = 100/\omega_0$. Frame grabbed at $t = 31.6/\omega_0$. [fig2.mov 2.5MB]

#85000 - $15.00 USD Received 9 Jul 2007; revised 14 Aug 2007; accepted 14 Aug 2007; published 15 Aug 2007

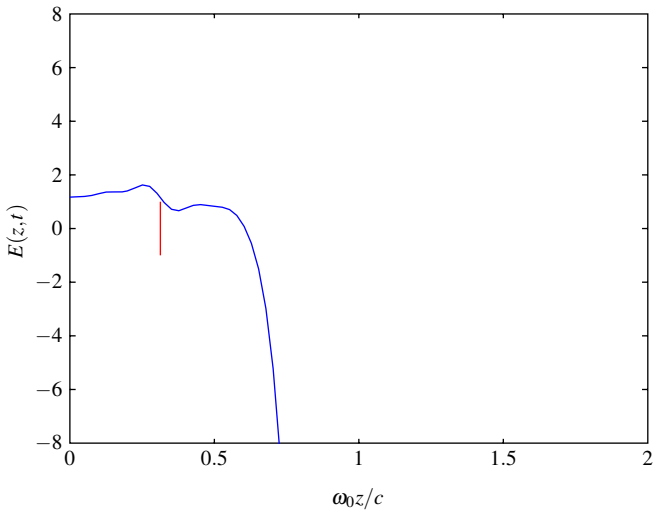

Fig. 3. Numerical simulation of $E(z,t)$ of a semi-infinite medium with $n(\omega) = n_1(\omega)$ and $\omega_1 = 1.4$. Frame grabbed at $t = 0.3/\omega_0$. Note that fields exist in front of the red line $z = ct$. The figure does not have the same axes and time scale as for Fig. 2. [fig3.mov 1.5MB]

the wave in Fig. 2 satisfies causality, while the wave in Fig. 3 does not. In fact, in Fig. 3 a nonzero field exists everywhere, even at $t = 0$. In Fig. 2, the wave front propagates at exactly the speed c [20]. Similarly, when the excitation is turned off, the high-frequency components induced by the abrupt envelope propagate at c. Note that the field eventually dies out after the excitation has been turned off. Some ripple can be seen in front of the red line in Fig. 2. This is a numerical error, which relate to Gibbs' effect, and can be reduced if a broader frequency representation is used.

To see that $n_1(\omega)$ not only gives a causal solution, but also the correct one, we compare the solution in Fig. 2 to the electromagnetic field in a slab of finite thickness d. Such a comparison makes sense since, by causality, the time-domain fields in a slab and in a semi-infinite medium must coincide for $t < d/c$. In an active slab, the fields may blow up with time and thus Fourier transformed fields may not exist. A natural remedy is to use Laplace transformed fields, i.e., to introduce complex frequencies with $\mathrm{Im}\,\omega > 0$. For a normally incident electromagnetic field, the reflected field R, the field in the slab $S = S^+\exp(ikz) + S^-\exp(-ikz)$, and the transmitted field T can be found as [11]

$$R = \frac{(\eta^2-1)\exp(-ikd) - (\eta^2-1)\exp(ikd)}{(\eta+1)^2\exp(-ikd) - (\eta-1)^2\exp(ikd)}, \tag{4a}$$

$$S^+ = \frac{2\eta(\eta+1)}{(\eta+1)^2 - (\eta-1)^2\exp(2ikd)}, \tag{4b}$$

$$S^- = \frac{2\eta(\eta-1)}{(\eta-1)^2 - (\eta+1)^2\exp(-2ikd)}, \tag{4c}$$

$$T = \frac{4\eta}{(\eta+1)^2\exp(-ikd) - (\eta-1)^2\exp(ikd)}. \tag{4d}$$

Note that R, S, and T are unchanged if $n \to -n$; thus the sign of n is irrelevant in Eq. (4). The time-domain field in the slab is computed by an inverse Laplace transform. The parameter γ must be chosen such that the integration path is located above all poles of S in the upper half-plane [23]. For the present choice of medium [$\varepsilon(\omega) = (1+f(\omega))^2$ and $\mu(\omega) = 1$], by choosing

#85000 - $15.00 USD Received 9 Jul 2007; revised 14 Aug 2007; accepted 14 Aug 2007; published 15 Aug 2007

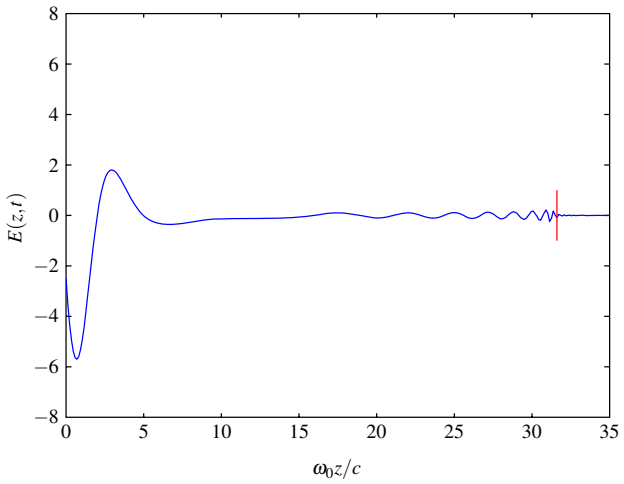

Fig. 4. Numerical simulation of $E(z,t)$ for a medium with $\varepsilon(\omega) = (1+f(\omega))^2$, $\mu(\omega) = 1$, finite thickness $\omega_0 d/c = 35$, and $\omega_1 = 1.4\omega_0$. The excitation is initiated at $t = 0$ and turned off at $t = 100/\omega_0$. The wave front $z = ct$ is indicated with a vertical red line. Frame grabbed at $t = 31.6/\omega_0$. [fig4.mov 3MB]

a sufficiently large $d < \infty$, it can be shown that there are no such poles. Then we can set $\gamma = 0^+$. We take the thickness to be $\omega_0 d/c = 35$, which in this case means that S does not have poles in the upper half-plane. The resulting time-domain field is given in Fig. 4. We clearly see that the solution in Fig. 4 equals the solution in Fig. 2 when $t < d/c$. Actually, the solutions are rather similar also for later times, which can be attributed to the fact that the field is small at $z = d$. Again we note that the field dies out after the excitation has been turned off; thus the excitation of the amplified "backward" wave in Fig. 4 is fundamentally different to conventional lasing.

We conclude that $n_1(\omega)$ is the correct refractive index function. The steady-state (monochromatic) solution, approached using the excitation $u(t)\cos(\omega_1 t)$ in the limit $t \to \infty$, demonstrates that the phase velocity points towards the source. Since $\mu = 1$, also the energy flow points towards the source. This backward wave draws energy from the active medium.

By analytic arguments, one can arrive at the same conclusion [11, 19]. Provided $\varepsilon\mu$ is continuous for real frequencies, one finds that the refractive index of (possibly) active media can be related to the permittivity and permeability using the formula

$$n = \sqrt{|\varepsilon||\mu|}\exp[i(\varphi_\varepsilon + \varphi_\mu)/2], \tag{5}$$

where $\varphi_\varepsilon + \varphi_\mu$ is the complex argument of $\varepsilon\mu$, unwrapped so that it is continuous and tends to zero as $\omega \to \infty$.

More generally, ε and μ may not be continuous for real frequencies (the Kramers–Kronig relations only imply analyticity in the upper half-plane $\operatorname{Im}\omega > 0$, not for $\operatorname{Im}\omega = 0$). Moreover, $\varepsilon\mu$ may contain odd-order zeros in the upper half-plane, which means that n cannot be identified as an analytic function there. Excluding the latter possibility (which corresponds to materials with so-called absolute instabilities [11]), we find the refractive index from the analytic branch of $\sqrt{\varepsilon\mu}$ that tends to $+1$ as $\operatorname{Im}\omega \to \infty$. The refractive index for real frequencies is the limit as $\operatorname{Im}\omega \to 0^+$ of this analytic branch. However, if $\varepsilon\mu$ contains only a single discontinuity or zero for real frequencies (at $\omega = 0$), we can still use Eq. (5), unwrapping in the frequency interval $(0,\infty)$, and ensuring the limit $\varphi_\varepsilon + \varphi_\mu \to 0$ as $\omega \to +\infty$.

The necessary phase unwrapping procedure means that the sign of the refractive index cannot

#85000 - $15.00 USD Received 9 Jul 2007; revised 14 Aug 2007; accepted 14 Aug 2007; published 15 Aug 2007

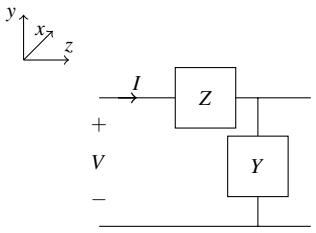

Fig. 5. A general transmission line representation.

be determined at a single frequency without knowing the global behavior of $\varepsilon(\omega)\mu(\omega)$ (at all frequencies). In other words, two media with $\varepsilon = 1 - i\alpha$, $\alpha > 0$ at a single frequency may have different refractive indices there. Thus the treatment of the example medium above does not contradict the fact that conventional gain media, with e.g. inverted Lorentzian responses, have positive real part of the refractive index. We note that any direct identification of n from ε and μ at a single frequency, such as in Refs. [13, 15, 17, 18], are incorrect in general.

It may seem that we have used causality as an extra principle in addition to Maxwell's equations, to calculate the field. However, causality is in fact built into the time-domain versions of the Maxwell equations: Provided ε and μ describe a microscopically causal medium (i.e., the polarization and magnetization do not precede the electric and magnetic fields), an electromagnetic excitation cannot give any response before the time z/c, where z is the distance between the excitation point and the observation point. Thus, one can actually verify Fig. 2 by solving Maxwell's equations in the time-domain, with no extra assumptions.

3. Effective medium based on a transmission line structure

The example in the previous section represents a novel class of active metamaterials [10, 11]. To realize this type of material both passive and active resonances are needed. An example of a typical passive resonance that fits this model is the serial RLC-resonance circuit. The inverted Lorentz function has similar behavior as a parallel RLC-resonance including an active element, which points us towards a transmission line with lumped element inclusions.

In 2002 Eleftheriades et. al. [5] proposed a negative index medium based on periodically L-C loaded transmission lines. As long as the periodicity of the structure remains less than roughly $\lambda_0/30$, where λ_0 is the vacuum wavelength [24], the structure can be described electromagnetically by an effective dielectric permittivity $\varepsilon\varepsilon_0$ $[\mathrm{F/m}]$ and an effective magnetic permeability $\mu\mu_0$ $[\mathrm{H/m}]$, where ε_0 and μ_0 are the vacuum permittivity and permeability. Consider a transmission line as shown in Fig. 5, with series impedance per length unit Z, and shunt admittance per length unit Y. The telegrapher's equation for a general 1-D transmission line can be expressed as:

$$\frac{\mathrm{d}V}{\mathrm{d}z} = -IZ, \tag{6a}$$

$$\frac{\mathrm{d}I}{\mathrm{d}z} = -VY. \tag{6b}$$

Combining Eqs. (6a) and (6b) yields

$$\frac{\mathrm{d}^2V}{\mathrm{d}z^2} + \beta^2 V = 0, \quad \beta^2 = -ZY, \tag{7}$$

where β is the propagation constant. Mapping the voltage V to E_y and the current I to $-H_x$ [5],

#85000 - $15.00 USD Received 9 Jul 2007; revised 14 Aug 2007; accepted 14 Aug 2007; published 15 Aug 2007

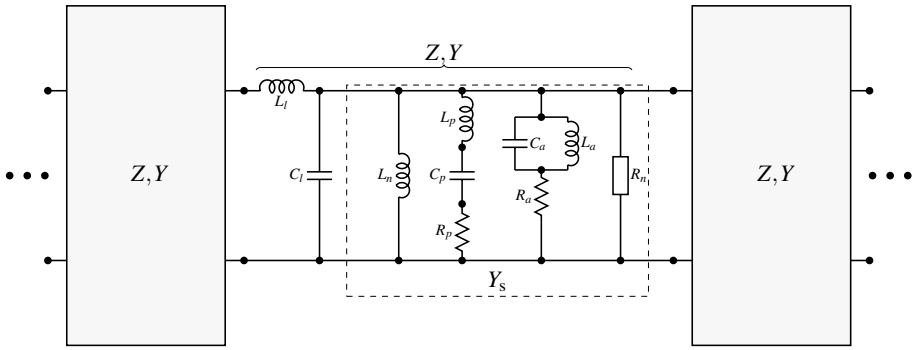

Fig. 6. Transmission line with additional shunt admittance Y_s.

Eqs. (6a) and (6b) can be rewritten as field equations:

$$\frac{\mathrm{d}E_y}{\mathrm{d}z} = -i\omega\mu\mu_0 H_x, \tag{8a}$$

$$\frac{\mathrm{d}H_x}{\mathrm{d}z} = -i\omega\varepsilon\mu_0 E_y, \tag{8b}$$

which yield the effective material parameters as

$$\mu = \frac{Z}{-i\omega\mu_0}, \tag{9a}$$

$$\varepsilon = \frac{Y}{-i\omega\varepsilon_0}. \tag{9b}$$

The propagation constant satisfies

$$\beta^2 = -ZY = \frac{\omega^2}{c^2}\varepsilon\mu. \tag{10}$$

It can easily be seen that interchanging the inductance and the capacitance of a conventional transmission line leads to negative ε and μ; thus the transmission line becomes left-handed. Since our goal is a right-handed transmission line medium with $\mu = 1$, we will leave the impedance inductive, $Z = -i\omega\mu_0$, and rather change the admittance Y so that ε becomes a sum of one passive and one active resonance [10, 25]. An example circuit is given in Fig. 6, where the total admittance is

$$Y = -i\omega C_l - \frac{1}{i\omega L_n} - \frac{i\omega/L_p}{\frac{1}{L_pC_p} - \omega^2 - i\omega\frac{R_p}{L_p}} + \frac{R_a+R_n}{R_aR_n}\frac{\frac{1}{L_aC_a} - \omega^2 - \frac{i\omega}{(R_a+R_n)C_a}}{\frac{1}{L_aC_a} - \omega^2 - \frac{i\omega}{R_aC_a}}. \tag{11}$$

Thus the effective relative permittivity and permeability become

$$\varepsilon(\omega) = \frac{1}{\varepsilon_0\Lambda}\left[C_l - \frac{1}{\omega^2 L_n} + \frac{1/L_p}{\frac{1}{L_pC_p} - \omega^2 - i\omega\frac{R_p}{L_p}} - \frac{R_a+R_n}{i\omega R_aR_n}\frac{\frac{1}{L_aC_a} - \omega^2 - \frac{i\omega}{(R_a+R_n)C_a}}{\frac{1}{L_aC_a} - \omega^2 - \frac{i\omega}{R_aC_a}}\right], \tag{12a}$$

$$\mu(\omega) = \frac{L_l}{\mu_0\Lambda}. \tag{12b}$$

#85000 - $15.00 USD Received 9 Jul 2007; revised 14 Aug 2007; accepted 14 Aug 2007; published 15 Aug 2007

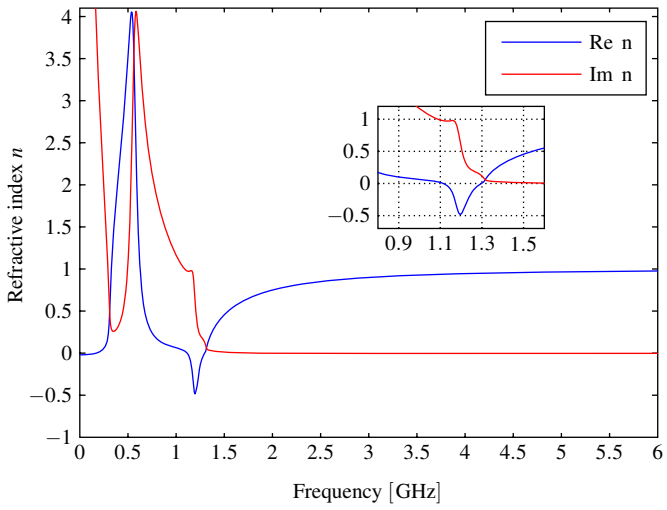

Fig. 7. Refractive index vs. frequency for the transmission-line effective medium.

Here Λ, C_l, and L_l are the length, capacitance, and inductance for a section of conventional transmission line; L_p, C_p, and R_p are the inductance, capacitance and resistance of the passive resonator; L_a, C_a, and R_a are the inductance, capacitance and resistance of the parallel resonator part of the circuit; R_n is the negative resistor element which provides gain. Negative resistance can be realized in several ways [26, 27]; transistors and Gunn-diodes are feasible alternatives. The parallel resonance has zero admittance at the resonance frequency. This acts together with the gain element to give negative admittance and negative imaginary part of the permittivity. The inductance L_n is included to remove a zero of ε from the positive imaginary frequency axis.

One must be careful when choosing the circuit parameters; it is not sufficient to have negative real part of the refractive index to obtain a medium similar to that in Section 2. It is important that ε does not have any odd-order zeros in the upper half plane, as this would create branch cuts in n. When there are such branch cuts, the refractive index loses its usual interpretation for real frequencies; moreover, the media are electromagnetically unstable (that is, with absolute instabilities, see [11]).

We have found that the following parameters will give negative refractive index in a small frequency window: $\Lambda = 6.25\,\mathrm{cm}$, $L_l = \mu_0\Lambda$, $C_l = \varepsilon_0\Lambda$, $R_n = -300\,\Omega$, $L_n = L_l$, $R_p = 20\,\Omega$, $L_p = 40\,\mathrm{nH}$, $C_p = 2\,\mathrm{pF}$, $R_a = 310\,\Omega$, $L_a = 1.8\,\mathrm{nH}$, and $C_a = 10\,\mathrm{pF}$. Figure 7 shows the refractive index versus frequency calculated by Eq. (5). Figure 8 shows the reflection coefficient calculated by Eq. (4a) using $d = 20\Lambda$. Negative real part of the refractive index exists in a small bandwidth from 1.11 GHz to 1.30 GHz, with the minimum value $\mathrm{Re}\,n = -0.48$ at 1.20 GHz. A maximum 2.1 of the reflection coefficient is attained at a slightly larger frequency. At 1.22 GHz the permittivity has positive real part, $\varepsilon = 0.0063 - 0.23i$, corresponding to $n = -0.34 + 0.33i$ and $|R| = 1.9$. The bandwidth where $\mathrm{Re}\,n < 0$ coincides with the bandwidth where $|R| > 1$.

4. Periodic structure

The effective medium theory yields a useful design guide for realization of the effective parameters as a transmission line with discrete elements. To investigate such periodic structures exactly, we use the transmission matrix method. The transmission matrix of a transmission line

#85000 - $15.00 USD Received 9 Jul 2007; revised 14 Aug 2007; accepted 14 Aug 2007; published 15 Aug 2007

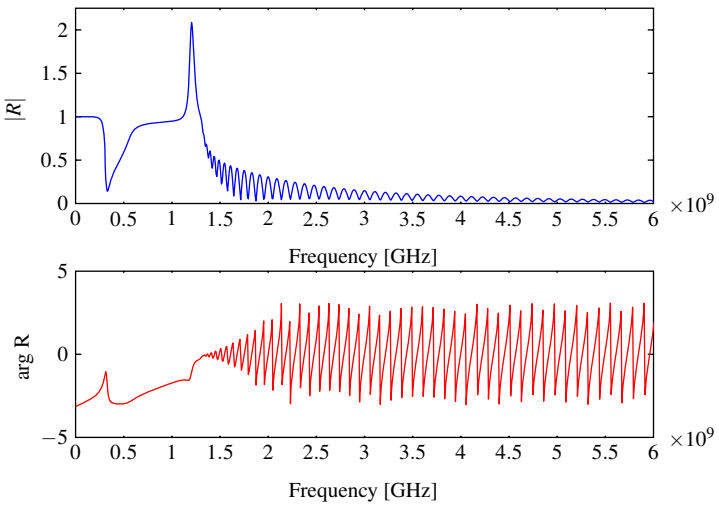

Fig. 8. R vs. frequency for total length $d = 20\Lambda$.

can be written [28]

$$T_{\mathrm{tl}} = \begin{bmatrix} \cos(\beta_0\Lambda) & -i\sin(\beta_0\Lambda)Z_0 \\ -i\sin(\beta_0\Lambda)/Z_0 & \cos(\beta_0\Lambda) \end{bmatrix}, \tag{13}$$

where Λ, $\beta_0 = \omega\sqrt{L_l C_l}$, and $Z_0 = \sqrt{L_l/C_l}$ are the length, propagation constant, and characteristic impedance, respectively. For a general shunt admittance Y_{s}, the transmission matrix is

$$T_{\mathrm{s}} = \begin{bmatrix} 1 & 0 \\ Y_{\mathrm{s}} & 1 \end{bmatrix}. \tag{14}$$

The transmission matrix for a unit cell is $T_{\mathrm{uc}} = T_{\mathrm{tl}}T_{\mathrm{s}}$, and the transmission matrix for N unit cells becomes

$$T = T_{\mathrm{uc}}^N = \begin{bmatrix} A & B \\ C & D \end{bmatrix}. \tag{15}$$

Since $\det T_{\mathrm{uc}} = 1$, the Nth power of T_{uc} can be calculated analytically with Chebyshev's identity [29]. T can now be converted into a scattering matrix [28]

$$S = \begin{bmatrix} S_{11} & S_{12} \\ S_{21} & S_{22} \end{bmatrix} = \begin{bmatrix} \dfrac{A+B/Z_0-CZ_0-D}{A+B/Z_0+CZ_0+D} & \dfrac{2(AD-BC)}{A+B/Z_0+CZ_0+D} \\ \dfrac{2}{A+B/Z_0+CZ_0+D} & \dfrac{-A+B/Z_0-CZ_0+D}{A+B/Z_0+CZ_0+D} \end{bmatrix}. \tag{16}$$

The scattering matrix element S_{11} is the reflection coefficient and S_{21} is the transmission coefficient. Note that S is symmetric due to reciprocity.

In the limit $N \to \infty$ while $d \equiv N\Lambda$ and Y_{s}/Λ are fixed, the transmission matrix model should correspond exactly to the effective medium theory. Indeed, we may expand T_{uc} to first order in Λ to obtain $T_{\mathrm{uc}} = I + \Upsilon\Lambda + \mathrm{O}(\Lambda^2) = \exp(\Upsilon\Lambda) + \mathrm{O}(\Lambda^2)$, where I is the identity matrix and

$$\Upsilon = \begin{bmatrix} 0 & -i\beta_0 Z_0 \\ -i\beta_0/Z_0 + Y_{\mathrm{s}}/\Lambda & 0 \end{bmatrix}. \tag{17}$$

Thus, in the above limit, $T = \exp(\Upsilon d)$, and analytical expressions for the scattering parameters S_{11} and S_{21} can be found and verified to be equal to Eqs. (4a) and (4d).

#85000 - $15.00 USD Received 9 Jul 2007; revised 14 Aug 2007; accepted 14 Aug 2007; published 15 Aug 2007

To analyze the behavior of the periodic structure for finite Λ, the fields are calculated for each unit cells of the periodic structure. This is achieved by first calculating the scattering matrix for the total structure and then utilizing the transmission matrix method to calculate the fields within the slab. Let the field (or voltage) incident to the structure be $V^+(\omega)$. The reflected voltage is $V^-(\omega) = V^+(\omega)S_{11}(\omega)$, and the voltage and current at the material interface are calculated as $V_1(\omega) = V^+(\omega) + V^-(\omega)$ and $I_1(\omega) = (V^+(\omega) - V^-(\omega))/Z_0$, respectively. Then the voltage and current in the next unit cell are given by

$$\begin{bmatrix} V_2(\omega) \\ I_2(\omega) \end{bmatrix} = T_{\text{uc}}^{-1} \begin{bmatrix} V_1(\omega) \\ I_1(\omega) \end{bmatrix}, \tag{18}$$

and so forth. (Since $\det T_{\text{uc}} = 1$, T_{uc} is invertible.) By standard inverse Laplace transforms, we finally find the time-domain fields at each unit cell of the structure.

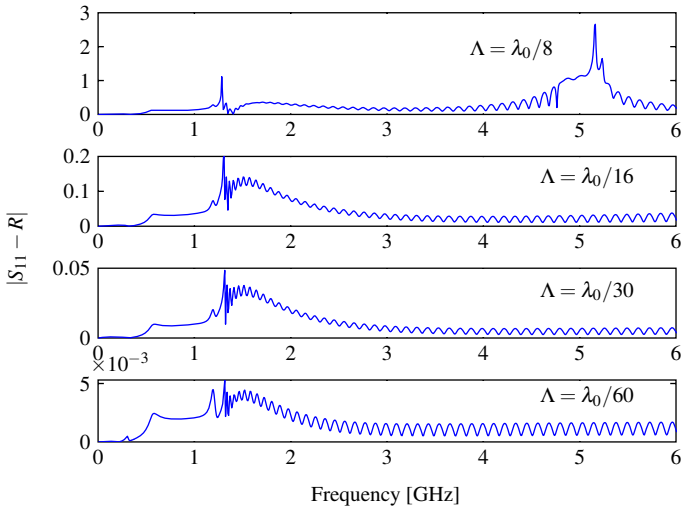

Fig. 9. $|S_{11} - R|$ vs frequency for $\Lambda = \lambda_0/8, \lambda_0/16, \lambda_0/30, \lambda_0/60$. $\lambda_0 = 25\,\text{cm}$ is the vacuum wavelength where $|R|$ is maximal.

Figure 9 shows the difference between the scattering parameter S_{11} for the periodic structure and the reflection coefficient R for the effective medium slab. The length scale Λ is varied while Y/Λ and $d = \Lambda N$ are fixed. To enable fair comparison, the reference plane of the periodic structure is shifted by an amount $\Lambda/2$ to the right, i.e., the periodic structure is symmetrized with respect to the point $z = d/2$. We see that there is a good agreement between the two calculations for $\Lambda = \lambda_0/30$ and even better when $\Lambda = \lambda_0/50$, as predicted by [24]. Figure 10 shows the time-domain field when exciting the periodic structure with the frequency $f_1 = 1.22\,\text{GHz}$. At this frequency the effective medium has $\varepsilon = 0.063 - 0.23i$. The excitation, $\cos(2\pi f_1 t)$, is initiated at $t = 0$ and shut off at $t = 20\,\text{ns}$. We observe that the forerunner propagates straight through the material at the vacuum light velocity. The backward wave builds up before the reflection from the far end has returned to the region near $z = 0^+$. After 20 ns the excitation is turned off. Then the associated transient propagates at c, and the backward wave dies out, demonstrating stability. This behavior is consistent with the example given in Sec. 2. We stress that we have analyzed a discrete lumped model with finite d; the scattering parameters are calculated by the transmission matrix method so that the refractive index is not considered.

The periodic circuit model is based on ideal passive components along with an ideal, constant negative resistor. For a more realistic model of the components it is possible to include resistive, capacitive and inductive parasitics into the components in use. Nevertheless, preliminary

#85000 - $15.00 USD Received 9 Jul 2007; revised 14 Aug 2007; accepted 14 Aug 2007; published 15 Aug 2007

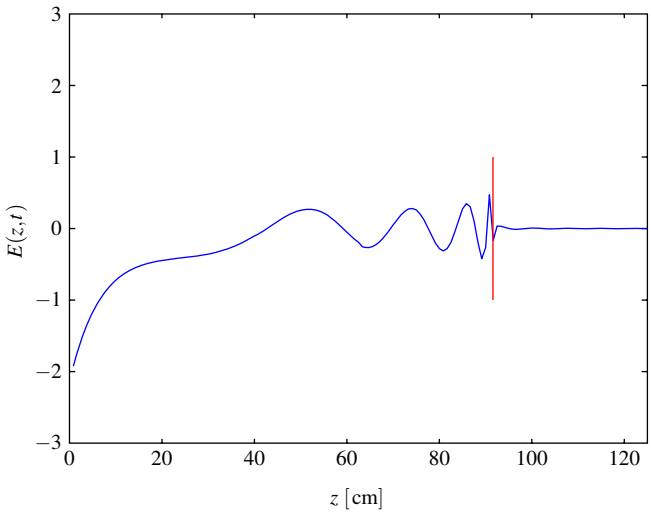

Fig. 10. Electrical field vs. distance and time, for a causal excitation $[u(t) - u(t - 20\,\text{ns})]\cos(2\pi f_1 t)$; $f_1 = 1.22\,\text{GHz}$, $d = 150\Lambda$, and $\Lambda = 0.83\,\text{cm}$. Frame grabbed at $t = 3.1\,\text{ns}$. [fig10.mov 3.4 MB]

sensitivity studies show that the circuit is not particularly sensitive to perturbations. The implementation of the negative resistor element should yield a broad-banded response compared to the two resonances.

5. Conclusion

We have presented theory and simulations which demonstrate how to determine the refractive index in active metamaterials. We have also proposed and analyzed a lumped circuit transmission line model for an active right-handed metamaterial with negative refractive index. This model demonstrates a backward propagating wave with phase velocity and Poynting's vector towards the source, and can be used as a starting point for implementation.

#85000 - $15.00 USD Received 9 Jul 2007; revised 14 Aug 2007; accepted 14 Aug 2007; published 15 Aug 2007